Cellular and Molecular Bioengineering, Vol. 14, No. 6, December 2021 *(© 2021)* pp. 639–651
https://doi.org/10.1007/s12195-021-00691-y

Original Article

The Impact of Astrocytes and Endothelial Cells on Glioblastoma Stemness Marker Expression in Multicellular Spheroids

PINAKI S. NAKOD, YONGHYUN KIM, and SHREYAS S. RAO

Department of Chemical and Biological Engineering, The University of Alabama, Tuscaloosa, AL 35487, USA

(Received 21 December 2020; accepted 12 July 2021; published online 20 July 2021)

Associate Editor Michael R. King oversaw the review of this article.

Abstract

Introduction—Glioblastoma multiforme (GBM), the most common primary brain tumor in adults, is extremely malignant and lethal. GBM tumors are highly heterogenous, being comprised of cellular and matrix components, which contribute to tumor cell invasion, cancer stem cell maintenance, and drug resistance. Here, we developed a heterotypic 3D spheroid model integrating GBM cells with astrocytes and endothelial cells (ECs) to better simulate the cellular components of the tumor microenvironment and investigate their impact on the stemness marker expression of GBM cells, which has not been previously investigated.

Methods—We used U87 GBM cells, C8-D1A mouse astrocytes, and human umbilical vein ECs to construct co- and triculture spheroid models in low-attachment U-well plates. We characterized the expression of known stemness markers NESTIN, SOX2, CD133, NANOG, and OCT4 in these models and compared it to respective mixed monoculture spheroids (control) using qRT-PCR and immunostaining.

Results—We incorporated GBM cells and astrocytes/ECs in 1:1, 1:2, 1:4, and 1:9 ratio and observed spontaneous self-assembled spheroids in all coculture conditions. We observed changing spheroid size dynamics over 7 days and an increased expression in stemness markers in GBM-astrocyte and GBM-EC coculture spheroids in 1:4 and 1:9 coculture conditions, respectively. In a triculture model employing GBM cells, astrocytes, and ECs in a 1:4:9 ratio, we found an increased expression of all the stemness markers.

Conclusions—We elucidated the impact of astrocytes and ECs on GBM stemness marker expression. This multicellular spheroid model may provide an important tool for investigating the crosstalk between cell types in GBM.

Keywords—Brain cancer, Cancer stem cells, Coculture, Triculture, Spheroids.

Address correspondence to Shreyas S. Rao, Department of Chemical and Biological Engineering, The University of Alabama, Tuscaloosa, AL 35487, USA. Electronic mail: srao3@eng.ua.edu

INTRODUCTION

Glioblastoma multiforme (GBM), the most common primary brain tumor, is extremely malignant. Despite the rigorous standard treatment involving radiation and chemotherapy, the average survival period is only 12-14 months from the time of diagnosis.[35] This can be, in part, attributed to the lack of understanding of the GBM tumor microenvironment. Thus, new approaches to study GBM behaviors *in vitro* are being developed by utilizing biomimetic culture systems that recapitulate key aspects of the complex *in vivo* tumor microenvironment.[34,41]

The GBM microenvironment is highly heterogenous and composed of not only tumor cells but also tumor-associated parenchymal cells such as astrocytes, endothelial cells (ECs), microglia, peripheral immune cells, and neural precursor cells. These cells contribute not only to tumor progression but also to more than 30% of the tumor mass.[42] ECs and astrocytes are components of the perivascular niche, which not only enhance tumor cell invasion but also support GBM-tumor initiating cells and/or induce de-differentiation of tumor cells to a tumor initiating (stem cell-like) phenotype.[37,42] Astrocytes were shown to enhance the invasion and migration of tumor cells by promoting the activity of matrix metalloproteinases and secretion of interleukin-6.[9,26] GBM tumors are highly vascularized, and angiogenesis, which is regulated by vascular endothelial growth factor (expressed by ECs), is essential to maintain rapid tumor growth.[34] Additionally, crosstalk between tumor cells and ECs has been shown to be governed by Notch signaling, which promotes angiogenic activity and stem cell maintenance.[37]

A subpopulation of GBM cells, expressing stemness-related markers like NESTIN, SOX2, CD133, NANOG and OCT4, have been reported to have stem

cell-like abilities such as self-renewal, multilineage differentiation, and heightened resistance to therapeutic treatments.[14,54] The tumor microenvironment provides signals that can alter stemness marker expression in tumor cells. These aspects have been investigated using several experimental models including *in vivo* mouse models, as well as emerging three-dimensional (3D) *in vitro* culture models vs. traditional two-dimensional (2D) tissue culture polystyrene (TCPS) cultures. For example, expression of stemness markers (CD133, CD15, NANOG, OLIG2, SHH, and EZH2) was enhanced in serum grown (more differentiated phenotype) GBM cells in a mouse model as a response to hypoxic and therapeutic stress.[3,11] Likewise, expression of stemness markers (NESTIN, SOX2, and CD133) was enhanced in 3D culture systems such as hyaluronic acid hydrogels, or electrospun polystyrene scaffolds compared to 2D TCPS cultures.[32,35]

GBM tumor cells have also been cultured as 3D multicellular tumor spheroids (MCTS) to study growth dynamics,[38] tumor invasion,[10] drug response,[1,13] as well as stemness marker changes.[19,51] MCTS have been commonly used as 3D *in vitro* models owing to the multiple advantages such as facilitation of cell organization in layers with different proliferation rates, presence of cell–cell interactions and signaling, and formation of nutrient and oxygen gradients.[25] However, few studies have examined the effects of coculturing astrocytes or ECs with GBM cells in a 3D MCTS model.[4,39,50] In addition, to the best of our knowledge, the effect of changing tumor and astrocyte/EC ratios on the stemness marker expression of GBM cells in a 3D MCTS co- and tri-culture model has not been reported.

Herein, we constructed 3D MCTS using serum grown GBM cells with astrocytes or ECs. We constructed a coculture MCTS model to evaluate the impact of varying coculture ratios (GBM cells: astrocytes/ECs) on the growth profile of spheroids and on the expression of stemness markers, particularly *NES*, *SOX2*, *CD133* (*PROM1*), *NANOG*, and *OCT4* (*POU5F1*). Further, we developed a triculture MCTS with GBM cells, astrocytes and ECs, and studied its growth dynamics as well as the expression of these stemness markers.

MATERIALS AND METHODS

Cell Culture

Human U87-MG GBM cells were cultured in Eagle's Minimum Essential Medium (EMEM; ATCC) supplemented with 10% fetal bovine serum (FBS) and 1% penicillin-streptomycin (VWR Life Science). Mouse astrocytes (C8D1A; ATCC) were kindly provided by Dr. Yuping Bao (Chemical and Biological Engineering, University of Alabama). Astrocytes were cultured in Dulbecco's Modified Eagle Medium (DMEM; Sigma Aldrich) supplemented with 10% FBS and 1% penicillin-streptomycin. Human umbilical vein endothelial cells (HUVECs, Lonza) were cultured in Endothelial Growth Medium-2 (EGM-2; Lonza) containing 2% FBS, supplements and growth factors per manufacturer's instructions (EGM-2 BulletKit; Lonza). All cells were maintained at 37 °C in a humidified 5% CO_2 environment and were harvested upon reaching 70–80% confluency using Trypsin (Gibco).

3D Monoculture MCTS

Monoculture MCTS were constructed according to the liquid overlay technique using a 96-well round bottom ultra-low attachment spheroid microplate (Corning®).[40] For construction of GBM-only spheroids, U87-MG cell suspensions were prepared in EMEM complete medium and 200 μL of cell suspensions corresponding to 500, 1000, 2500, 5000, 7500 and 10,000 cells/well, was transferred into each well. After cell seeding, plates were centrifuged at 1000×*g* for 10 min and incubated at 37 °C in a humidified 5% CO_2 environment. The monoculture MCTS were cultured up to day 7 and half the medium was replenished every 2 days. Similarly, astrocytes-only and EC-only spheroids were prepared using 5000, 10,000, 20,000, 45,000 cells/well.

Construction of 3D Coculture MCTS

Coculture MCTS were constructed similarly to monoculture MCTS. To identify astrocytes or ECs within a coculture MCTS, the dissociated single cells were first labeled with CellTracker fluorescent probes, green CMFDA dye (Invitrogen), before seeding.[35] Suspensions of each cell type were prepared in their respective complete medium and 100 μL of each cell suspension was transferred into each well. GBM-astrocytes and GBM-EC coculture MCTS were maintained in 1:1 EMEM:DMEM and 1:1 EMEM:EGM-2 media composition, respectively. The resulting composition was such that GBM:astrocytes and GBM:EC were seeded at 1:1, 1:2, 1:4 and 1:9 ratios, where the number of U87-MG cells were fixed at 5000 cells/well and only the number of astrocytes or EC were changed. The coculture MCTS were cultured up to day 7.

Construction of 3D Triculture MCTS

Triculture MCTS comprising of U87-MG, C8D1A and HUVECs were constructed similarly as above. To identify the different cells within the MCTS, U87-MG cells and astrocytes were labeled with red and green CellTracker dyes. Suspensions of each cell type were prepared in their respective complete medium and 67 μL of each cell suspension was transferred into a well. This GBM-astrocytes-HUVEC triculture MCTS was maintained in 1:1:1 EMEM:DMEM:EGM-2 media composition. The resulting composition was such that GBM:astrocytes:EC were seeded at a ratio of 1:4:9, where the number of U87-MG cells were fixed at 5000 cells/well. The triculture MCTS were also cultured up to day 7.

Optical Fluorescence Microscopy and Image Analysis

The spheroids were monitored using an Olympus IX83 microscope with a spinning disc confocal attachment. Representative brightfield and fluorescent images for day 1 were collected ~ 24 h after the cells were initially seeded and the plate was centrifuged. Brightfield and fluorescent images were also collected at day 4 and 7. The size and the cross-sectional area of the spheroids were analyzed using ImageJ software (NIH).[35] At day 1, 4 and 7, visual assessment of the compactness of spheroids was done based on a previously described 5-point scale.[28] The scores were allocated by three blinded researchers based on the structure of the spheroids and the averages were presented.

Quantitative Real-Time Polymerase Chain Reaction (qRT-PCR)

qRT-PCR was performed on RNA samples obtained from GBM-astrocytes and GBM-EC coculture MCTS and compared to RNA samples comprised of a mixture of RNA from the GBM-only and astrocytes-only or EC-only monoculture MCTS as described previously (Fig. S1).[37] The samples were combined such that the initial cell seeding densities of the monoculture spheroids matched the initial cell density of the coculture spheroid in terms of number of individual cells and ratio of GBM:astrocytes or GBM:EC. Similar protocol was followed for triculture MCTS.

To assess the marker expression at day 7, 3-5 spheroids per replicate were harvested using p200 pipette with tip cut halfway to facilitate easy removal of spheroids while preserving their integrity and were pooled. RNA was extracted and transcribed into cDNA for quantification as described previously.[35] The primers used are provided in Table S1. Relative expression of the genes compared to the housekeeping gene (GAPDH) were calculated using $\Delta\Delta C_t$ method, where $\Delta C_t = \Delta C_{t,\text{gene of interest}} - \Delta C_{t,GAPDH}$. Coculture and triculture data was normalized to the respective mixed cultures.

Immunofluorescence Staining

On day 7, 3-5 monoculture, coculture and triculture spheroids were dissociated into single cells by adopting the procedure described previously.[23] Immunofluorescence staining was performed on single cells obtained from GBM-astrocytes coculture MCTS, GBM-EC coculture MCTS, and triculture MCTS. These were compared to single cells obtained from a mixture of (a) GBM-only and astrocytes-only monoculture MCTS, (b) GBM-only and EC-only monoculture MCTS, and (c) GBM-only, astrocytes-only, and EC-only monoculture MCTS, respectively. The dissociated single cells were transferred to a 96-well plate and then fixed with 4% paraformaldehyde, permeabilized using 0.25% Triton-X in 1× phosphate buffered saline (PBS) and blocked with 5% bovine serum albumin (BSA) in 1× PBS. The cells were incubated overnight at 4 °C with primary antibodies diluted as per manufacturer's protocol (Table S2). The cells were then incubated with Alexa Fluor 594-conjugated goat anti-rabbit secondary antibody (A-11012, Invitrogen) at 4 °C for 1 h the following day and counterstained with DAPI nuclear stain for 5 min. The plate was centrifuged at ~1000×g for ~ 15 s every time prior to the removal of liquids from wells to avoid the loss of cells. The cells were then imaged using an Olympus IX83 microscope with a spinning disc confocal attachment. To identify the different cell types in co- and tri-culture MCTS, one of the cell types was labeled with CellTracker™ Green CMFDA dye while constructing the spheroids. Cells with no green signal and positive red and blue signal were identified as tumor cells positive for the corresponding marker for GBM-astrocyte MCTS. Cell with a positive green, red, and blue signal were identified as tumor cells positive for the corresponding marker for GBM-EC or triculture MCTS. Percentage positive tumor cells were evaluated through manual counting using multi-point tool in ImageJ software (NIH) as previously described.[23,36]

Statistical Analysis

The data is presented as mean ± standard error unless mentioned otherwise. Statistical analysis was performed with JMP® software and the significance was calculated using Student's t-test or analysis of variance followed by Tukey's HSD *post-hoc* analysis.

All the experiments were repeated independently at least twice. With all analyses, the significance level was set at $p \leq 0.05$.

RESULTS

Construction and Characterization of 3D MCTS

MCTS consisting of GBM-only, astrocytes-only, or EC-only were constructed according to the liquid overlay technique. We utilized U87-MG cells to prepare GBM-only spheroids with initial seeding densities of 500, 1000, 2500, 5000, 7500, and 10000 cells/well (Fig. S2). At day 1, U87-MG cells in all the conditions spontaneously arranged themselves to form a loosely aggregated spheroid, and the spheroid sizes significantly increased ($p \leq 0.05$) from day 1 to day 7. Spheroids made from 500 and 1000 cells showed similar areas on days 1, 4, and 7, as well as the highest increase ($p \leq 0.05$) from day 1 to day 7 by 7.6-fold and 4.8-fold, respectively. Interestingly, despite the difference in the initial seeding density in 5000, 7500 and 10000 cells/well conditions, almost similar sized spheroids were observed at days 1, 4 and 7. The spheroids made from 5000 cells/well showed an increase of 1.8-fold and 1.9-fold from day 1 to day 4 and day 4 to day 7, respectively ($p \leq 0.05$). We chose spheroids made with 5000 cells/well for subsequent experiments and these were used as controls in co- and tri-culture MCTS models.

We utilized mouse astrocyte cell line C8D1A and HUVECs to prepare monoculture MCTS and in co- and tri-culture MCTS models to mimic tumor-stroma interactions. We prepared astrocytes-only or EC-only spheroids by seeding the cells at initial seeding densities of 5000, 10000, 20000, and 45000 cells/well (Figs. S3, S4). For both cell types, the size of the spheroids decreased with time. The spheroid growth profile and trends of astrocytes-only and EC-only spheroids were similar at days 1, 4 and 7. To incorporate tumor-stroma interactions, we constructed coculture MCTS with tumor cells at fixed initial seeding density of 5000 cells/well and only increasing the initial seeding density of astrocytes or ECs resulting in coculture ratios of 1:1, 1:2, 1:4, and 1:9.

GBM-Astrocytes Coculture MCTS

For all the coculture conditions, majority of the tumor cells and astrocytes spontaneously self-assembled to form a loosely aggregated spheroid at day 1 (Fig. 1a). At day 1, significantly different ($p \leq 0.05$) spheroid sizes were observed for all coculture conditions and control (Fig. 1b). At day 4, all the coculture conditions (except 1:1) showed significant decrease ($p \leq 0.05$) in spheroid size compared to day 1. From day 1 to day 4, significant decrease ($p \leq 0.05$) of 2-fold, 1.9-fold, 1.5-fold was observed for 1:9, 1:4 and 1:2 coculture spheroids, respectively, and slight decrease of 0.9-fold was observed for 1:1 coculture spheroids ($p > 0.05$). At day 4, similar spheroid sizes were observed for the lower coculture ratio conditions (1:1 and 1:2; $p > 0.05$) and significantly larger spheroid sizes ($p \leq 0.05$) were observed for 1:9 followed by 1:4 coculture spheroids. All coculture spheroids continued to grow as indicated by the significant increase in sizes from day 4 to day 7 ($p \leq 0.05$). This increase was 1.7-fold, 1.6-fold, 1.6-fold and 1.2-fold for 1:1, 1:2, 1:4 and 1:9 GBM-astrocytes coculture spheroids, respectively. Overall, from day 1 to day 7, we observed a decrease of 1.7-fold for 1:9 coculture condition ($p \leq 0.05$), 1.2-fold for 1:4 coculture condition ($p \leq 0.05$), no change for 1:2 coculture condition ($p > 0.05$), and an increase of 1.7-fold for 1:1 coculture condition ($p \leq 0.05$). The compactness of all coculture MCTS significantly increased with time from day 1 to day 7 (Fig. S5A). GBM-only control spheroids showed an increasing size trend with time consistent with earlier observations. In spite of the differences in the initial seeding densities, at day 7, similar spheroid sizes were observed for all the coculture conditions as well as control (except 1:2 coculture spheroids which were significantly smaller compared to other conditions). Pre-labeling the astrocytes allowed observation of cell–cell stratification within the spheroid; and astrocytes were seen to mostly occupy the spheroid core (Fig. S6).

GBM-EC Coculture MCTS

Similar to the GBM-astrocytes MCTS, majority of the tumor and ECs spontaneously self-assembled to form a loosely aggregated spheroid for all the coculture conditions at day 1 (Fig. 2a). At day 1, significantly different ($p \leq 0.05$) spheroid sizes were observed for all coculture conditions and control (Fig. 2b). Unlike GBM-astrocytes coculture MCTS where significant decrease in sizes were observed for all the conditions; for GBM-EC coculture spheroids, an increase in spheroid sizes was observed for lower coculture ratio conditions (1:1 and 1:2) and decrease in spheroid sizes was observed for higher coculture ratio conditions (1:4 and 1:9). As compared to day 1, significant increase ($p \leq 0.05$) of 1.5-fold and 1.3-fold were observed for 1:1 and 1:2 coculture spheroids, respectively at day 4. For the higher coculture conditions, a decrease of 1.4-fold and 0.9-fold was observed for 1:9 and 1:4 coculture spheroids, respectively at day 4. At day 4, similar spheroid sizes were observed for 1:1, 1:2 and 1:4 coculture conditions, with 1:9 condition having significantly larger spheroids ($p \leq 0.05$) than other con-

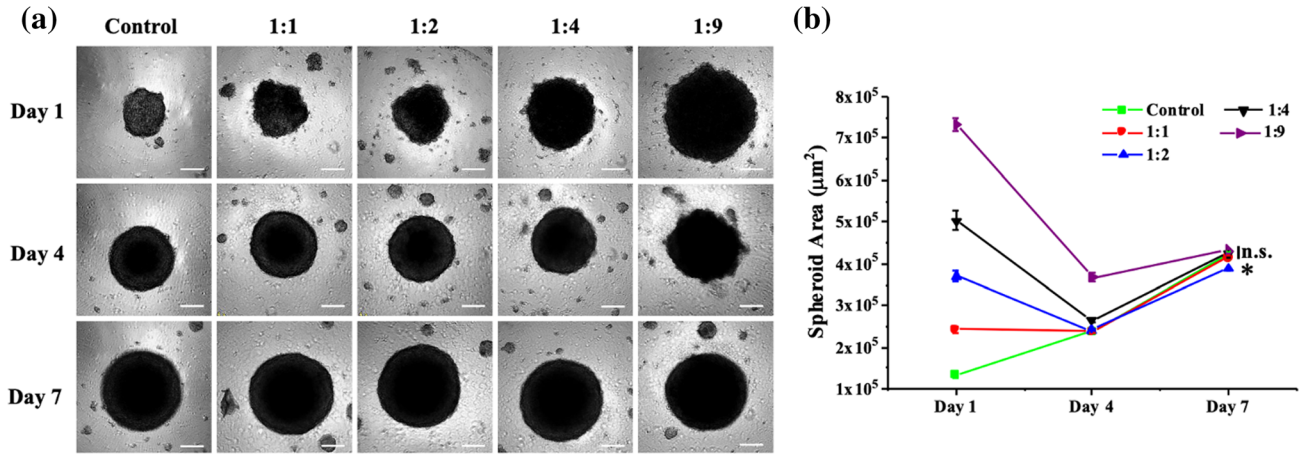

FIGURE 1. Characterization of 3D GBM-astrocyte coculture MCTS. (a) Representative brightfield images of GBM cells cocultured with astrocytes at a ratio of 1:1, 1:2, 1:4 and 1:9 and GBM-only cells (control) at days 1, 4, and 7 post-seeding. Scale bar = 200 μm. (b) Quantification of spheroid areas over time for all GBM-astrocyte coculture conditions. Values represent mean ± standard error. N ≥ 9 replicates per condition. *$p \leq 0.05$ for 1:2 coculture condition compared to other conditions.

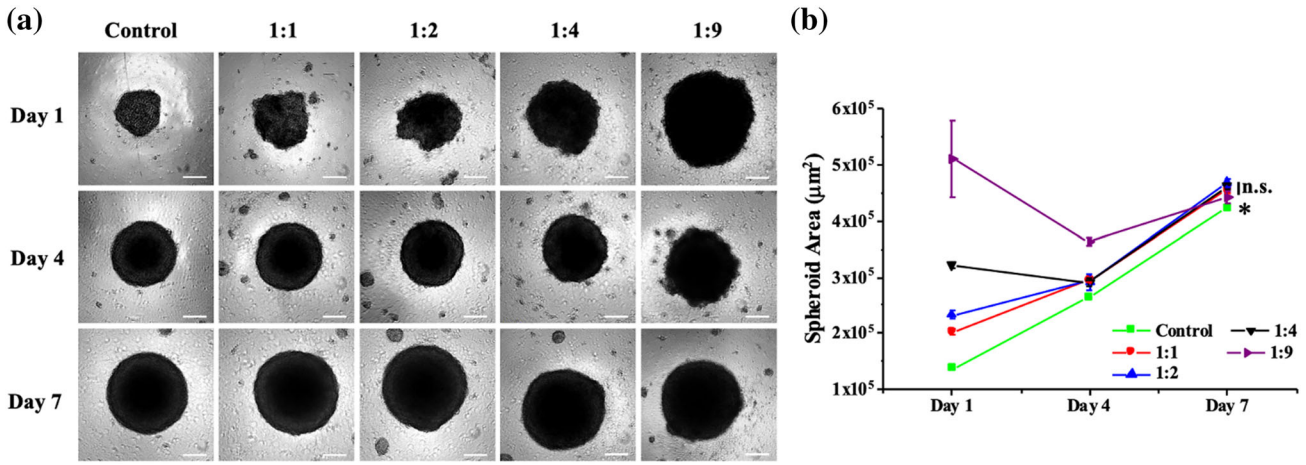

FIGURE 2. Characterization of 3D GBM-EC coculture MCTS. (a) Representative brightfield images of GBM cells cocultured with ECs at a ratio of 1:1, 1:2, 1:4 and 1:9 and GBM-only cells (control) at days 1, 4, and 7 post-seeding. Scale bar = 200 μm. (b) Quantification of spheroid areas over time for all GBM-EC coculture conditions. Values represent mean ± standard error. N ≥ 9 replicates per condition. *$p \leq 0.05$ for control compared to other conditions.

ditions. All coculture spheroids continued to grow as indicated by the significant increase in size from day 4 to day 7 ($p \leq 0.05$). At day 7, except for 1:9 coculture condition with 1.2-fold increase, an increase of 1.6-fold was observed for all the other conditions as compared to day 4. Overall, from day 1 to day 7, we observed a significant increase ($p \leq 0.05$) of 1.4-fold, 2-fold and 2.2-fold for 1:4, 1:2 and 1:1 coculture conditions, respectively, and a decrease of 1.2-fold for 1:9 coculture condition ($p \leq 0.05$). The compactness of all coculture MCTS significantly increased with time from day 1 to day 7 (Fig. S5B). GBM-only control spheroids showed an increasing size trend with time consistent with earlier observations. In spite of the differences in the initial seeding densities, at day 7, similar spheroid sizes were observed for all GBM-EC coculture conditions except control spheroids which were significantly smaller compared to others. Pre-labeling ECs allowed observation of cell–cell stratification within the spheroid; and similar to astrocytes, even the ECs were seen to mostly occupy the spheroid core (Fig. S7).

Stemness Marker Expression of Tumor Cells in 3D Coculture MCTS

We investigated how astrocytes and ECs influence the expression of *NES*,[48] *SOX2*,[17] *CD133*,[17] *NANOG*,[6] and *OCT4*[6] as these markers have been most commonly used for the identification of stemness phenotype in glioblastoma cells.[54] Specifically, we assessed the stemness marker expression of tumor cells cocultured in direct contact with astrocytes/ECs in different

coculture ratios (1:1, 1:2, 1:4 and 1:9), and compared them to the respective individually cultured and mixed tumor cells and astrocytes/ECs counterparts (Mixed GBM-astrocytes or Mixed GBM-EC) at day 7 (Fig. S1).

GBM-Astrocytes Coculture MCTS

After culturing the tumor cells with astrocytes in a coculture MCTS model for 7 days, significant increase ($p \leq 0.05$) in the expression of *NES* by 2.6-fold was observed for the 1:4 condition. The expression of *NES* was increased by 1.6-fold in 1:9 condition ($p > 0.05$) and almost unaltered in the 1:1 and 1:2 conditions ($p > 0.05$) (Fig. 3a). The expression of *SOX2* significantly decreased ($p \leq 0.05$) for the 1:1 and 1:2 condition by 5-fold and 3.7-fold, respectively (Fig. 3b). No significant changes in the expression of *SOX2* were observed at higher coculture ratios—1:4 and 1:9. *CD133* expression increased significantly ($p \leq 0.05$) by 2.7-fold and 2.5-fold for 1:4 and 1:9 conditions, respectively, and remained unaltered ($p > 0.05$) in the lower coculture ratio conditions (Fig. 3c). Although, an increase in *NANOG* expression of 2.3-fold and 2.1-fold was observed for 1:4 and 1:9 conditions, no statistically significant changes were observed for any of the conditions (Fig. 3d). The trends for *OCT4* were similar to *NES*, where significant increase ($p \leq 0.05$) by 2.3-fold was observed for 1:4 condition (Fig. 3e). Also, the expression of *OCT4* was increased by 1.6-fold in 1:9 condition ($p > 0.05$) and almost unaltered in the lower coculture ratio conditions (1:1 and 1:2; $p > 0.05$). Overall, the most prominent changes in the expression of stemness markers were observed for 1:4 GBM-astrocyte coculture spheroid. We then evaluated the expression these markers at the protein level for 1:4 GBM-astrocyte coculture MCTS through immunofluorescence staining. We observed a significant increase ($p \leq 0.05$) in the percentage of NESTIN-positive, SOX2-positive, and OCT4-positive tumor cells in 1:4 GBM-astrocyte coculture MCTS compared to the control (i.e., mixture of GBM-only and astrocyte-only monoculture MCTS) (Figs. S8, S9 and S12). However, the percentage of CD133-positive and NANOG-positive tumor cells was similar (Figs. S10 and S11).

GBM-EC Coculture MCTS

After culturing the tumor cells with ECs in a coculture MCTS model for 7 days, significant increase ($p \leq 0.05$) in the expression of *NES* by 2.5-fold and 4.9-fold was observed for 1:4 and 1:9 conditions, respectively (Fig. 4a). In the lower coculture ratio conditions, 1:1 and 1:2, no significant changes in *NES* expression were observed although an increase of 2.2-fold was observed for the 1:2 condition. The expression of *SOX2* significantly increased ($p \leq 0.05$) for the higher coculture ratio conditions, 1:4 and 1:9, by 2.7-fold and 6.1-fold, respectively (Fig. 4b). In the lower coculture ratio conditions, 1:1 and 1:2, no significant changes in

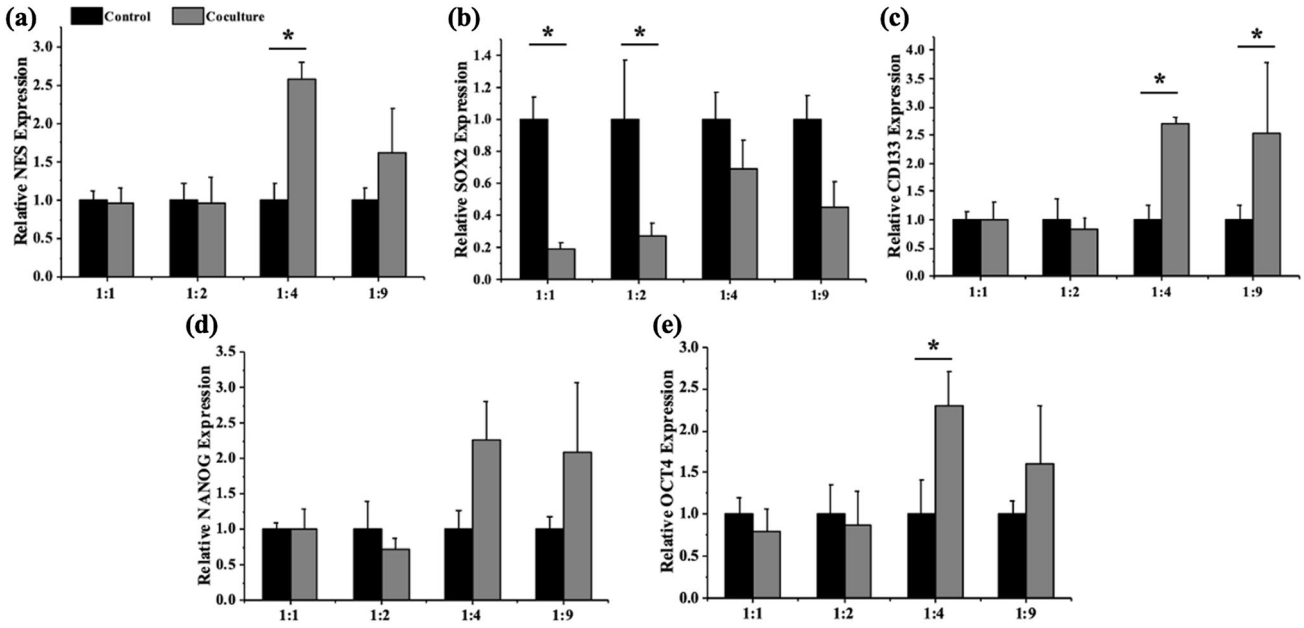

FIGURE 3. Astrocytes influence expression of stemness markers in a 3D GBM-astrocyte coculture MCTS model. Relative expression of (a) *NES*, (b) *SOX2*, (c) *CD133*, (d) *NANOG*, and (e) *OCT4* in 1:1, 1:2, 1:4 and 1:9 GBM-astrocyte coculture conditions. Relative expression normalized to the respective mixed GBM-astrocyte control. Values represent mean ± standard error. N = 3 biological replicates per condition which were independently setup. *$p \leq 0.05$ compared to the respective mixed GBM-astrocyte control.

SOX2 expression were observed although an increase of 1.9-fold was observed for 1:2 condition ($p > 0.05$). Increased expression of *CD133* was observed for all the conditions, however, was statistically significant ($p \leq 0.05$) only for 1:9 condition with an increase of 3.5-fold (Fig. 4c). Similarly, an increased expression of *NANOG* was observed for all the conditions, however, was statistically significant ($p \leq 0.05$) only for 1:2 and 1:9 conditions with an increase of 1.7-fold and 3.4-fold, respectively (Fig. 4d). An increased expression trend of *OCT4* was observed for all conditions, however, was statistically significant ($p \leq 0.05$) only for 1:9 condition with an increase of 3-fold (Fig. 4e). Overall, the most prominent changes in the expression of stemness markers were observed for 1:9 GBM-EC coculture MCTS. We then evaluated the expression these markers at the protein level for 1:9 GBM-EC coculture MCTS through immunofluorescence staining. We observed a significant increase ($p \leq 0.05$) in the percentage of NESTIN-positive, SOX2-positive, and CD133-positive tumor cells in 1:9 GBM-EC coculture MCTS compared to the control (i.e., mixture of GBM-only and EC-only monoculture MCTS) (Figs. S13, S14 and S15). However, the percentage of NANOG-positive and OCT4-positive tumor cells was similar (Figs. S16 and S17).

3D Triculture MCTS

Next, we established a triculture MCTS model by culturing tumor cells with astrocytes and ECs. To the best of our knowledge, this is the first time these three cell types have been combined in a MCTS model. The most effective coculture ratio in terms of prominent changes in stemness marker expression was chosen from coculture studies. Tumor cells were cultured with astrocytes and ECs in the ratio of 1:4:9 where the initial number of tumor cells was fixed at 5000 cells/well. GBM-only spheroids made with an initial seeding density of 5000 cells/well served as control.

Construction and Characterization of 3D Triculture MCTS

All the cell types with different initial seeding densities spontaneously arranged themselves to form a loosely aggregated spheroid at day 1 (Fig. 5a). Similar to the coculture MCTS, a significant decrease ($p \leq 0.05$) of 1.5-fold was observed from day 1 to day 4, after which the spheroid size significantly increased ($p \leq 0.05$) by 1.2-fold at day 7 (Fig. 5b). There was a significant decrease ($p \leq 0.05$) of 1.3-fold from day 1 to day 7. Similar to coculture MCTS, compactness of triculture MCTS significantly increased with time from day 1 to day 7 (Fig. S5C). GBM-only control spheroids showed an increasing size trend with time consistent with earlier observations. Pre-labeling the tumor cells

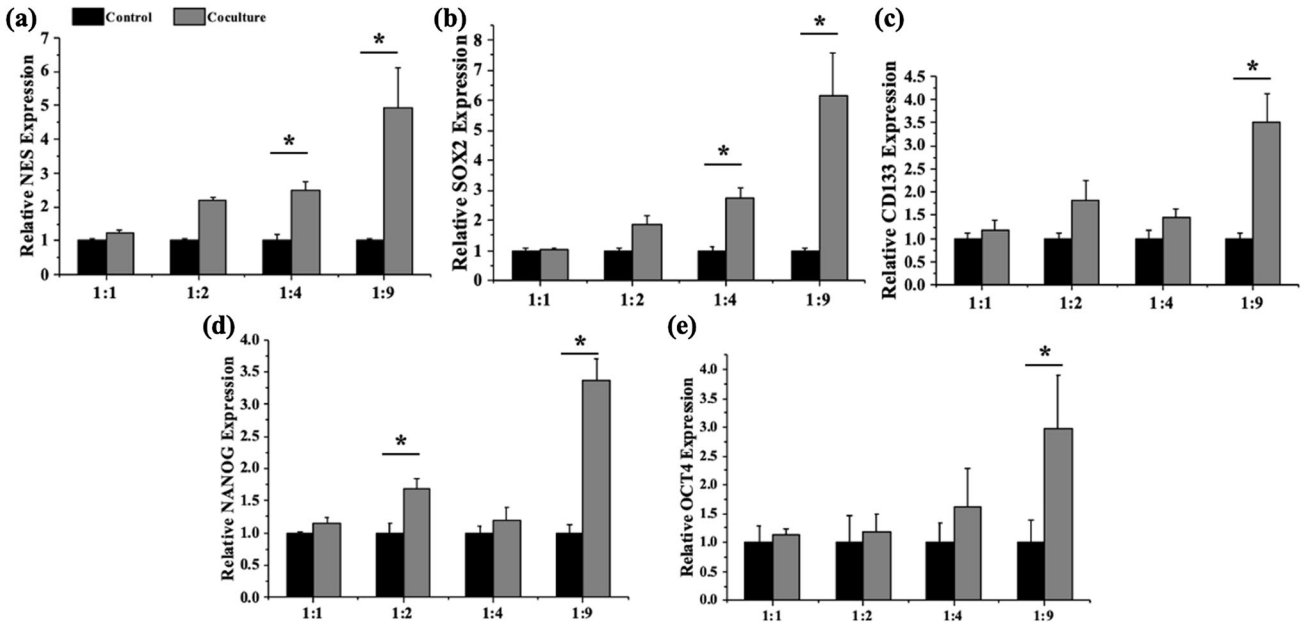

FIGURE 4. Endothelial cells influence expression of stemness markers in a 3D GBM-EC coculture MCTS model. Relative expression of (a) *NES*, (b) *SOX2*, (c) *CD133*, (d) *NANOG*, and (e) *OCT4* in 1:1, 1:2, 1:4 and 1:9 GBM-EC coculture conditions. Relative expression normalized to the respective mixed GBM-EC control. Values represent mean ± standard error. N = 3 biological replicates per condition which were independently setup. *$p \leq 0.05$ compared to the respective mixed GBM-EC control.

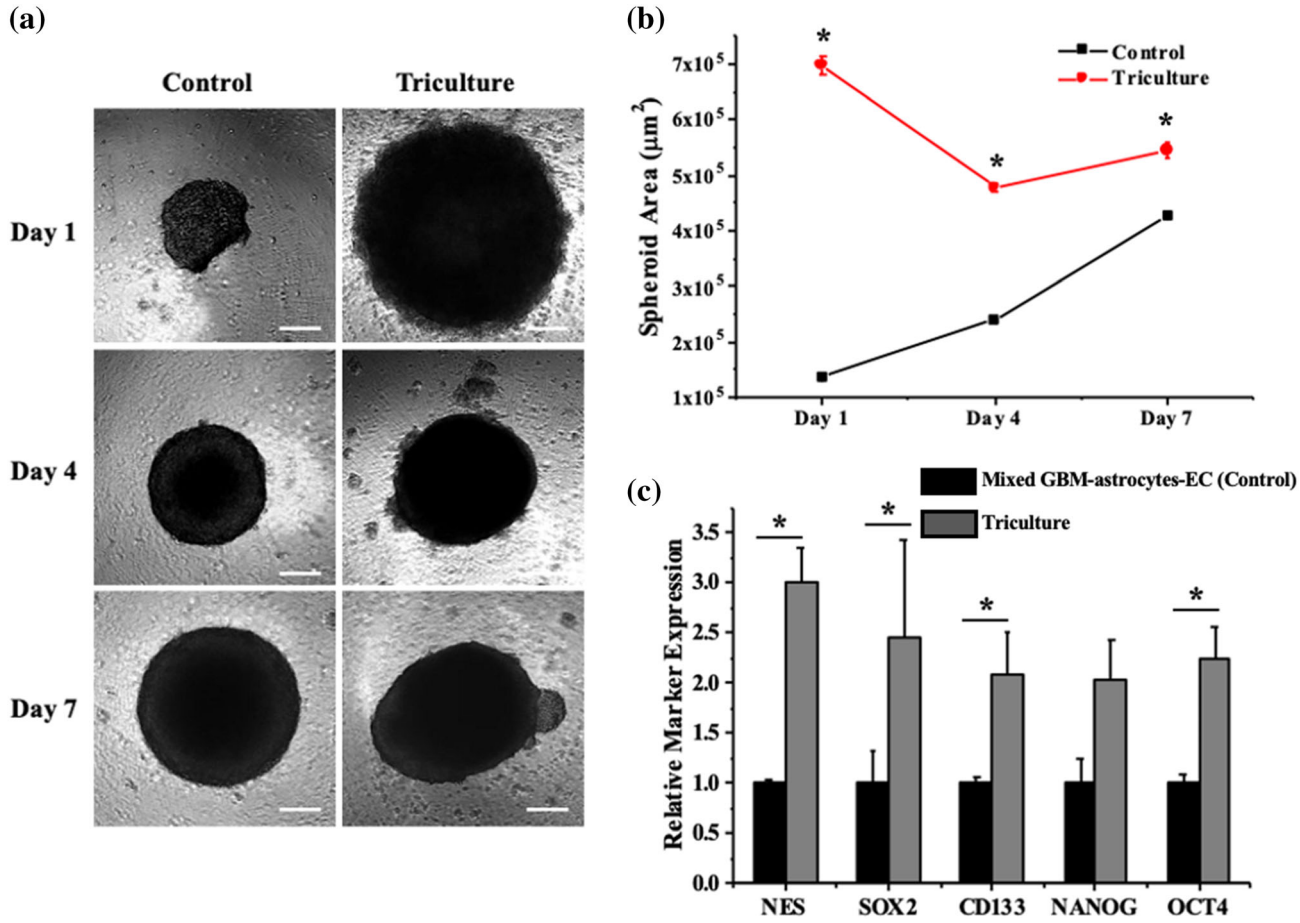

FIGURE 5. Characterization of 3D triculture MCTS incorporating GBM cells, astrocytes and ECs at a ratio of 1:4:9. (a) Representative brightfield images of triculture and GBM-only (control) spheroids at days 1, 4, and 7 post-seeding. Scale bar = 200 μm. (b) Quantification of spheroid areas over time for triculture and GBM-only (control) spheroids. *$p \leq 0.05$ compared to GBM-only (control). (c) Relative expression of stemness markers—*NES*, *SOX2*, *CD133*, *NANOG*, and *OCT4* normalized to the mixed GBM-astrocyte-ECs (control). Values represent mean ± standard error. N = 3 biological replicates per condition which were independently setup. *$p \leq 0.05$ compared to the respective mixed GBM-astrocyte-ECs (control).

and astrocytes allowed the observation of cell–cell stratification within the spheroid (Fig. S18).

Stemness Marker Expression of Tumor Cells in 3D Triculture MCTS

We assessed the stemness marker expression of tumor cells cultured with astrocytes and ECs in the ratio of 1:4:9 (Triculture MCTS) and compared them to the respective individually cultured and mixed spheroids of tumor cells, astrocytes, and ECs at day 7. The effect of disparate cell populations on differential gene expression results was minimized by constructing RNA samples with similar cellular compositions. This allowed us to investigate the effect of culturing tumor and stromal cells in direct contact in triculture MCTS compared to the segregated monoculture MCTS of these cell types. After culturing the tumor cells with astrocytes and ECs in the triculture MCTS model for 7 days, a significant increase was observed in the expression of *NES*, *SOX2*, *CD133*, and *OCT4* by 3-fold, 2.4-fold, 2.1-fold and 2.2-fold, respectively ($p < 0.05$) (Fig. 5c). Although, the *NANOG* expression increased by 2-fold, the increase was not statistically significant. Overall, the stemness marker expression of tumor cells was enhanced when cultured with stromal cells in a triculture MCTS. We then evaluated the expression these markers at the protein level for the triculture MCTS through immunofluorescence staining. We observed a significant increase ($p \leq 0.05$) in the percentage of NESTIN-positive, SOX2-positive, and CD133-positive tumor cells in the triculture MCTS compared to the control (i.e., mixture of GBM-only, astrocyte-only and EC-only monoculture MCTS) (Figs. S19, S20 and S21). We observed an increase in the percentage of NANOG-positive and OCT4-positive tumor cells, however it was not statistically significant ($p > 0.05$) (Figs. S22 and S23).

DISCUSSION

In this study, we constructed 3D co- and tri-culture MCTS to study the impact of astrocytes and ECs on the stemness marker expression of GBM cells. We evaluated changes in stemness marker expression with respect to changing coculture ratios of tumor cells and astrocytes/ECs in a coculture MCTS model and also developed a triculture MCTS model consisting of tumor cells, astrocytes, and ECs. So far, few studies have employed spheroid-based models to coculture GBM cells (serum grown; more differentiated phenotype) with astrocytes/ECs. Also, to the best of our knowledge, comparison of the stemness marker expression with changing ratios of GBM to astrocytes/ECs has not been previously evaluated in a relevant 3D MCTS model. Through this study, we are bridging the gap by constructing co- and tri-culture MCTS models with GBM cells, astrocytes and ECs to study the effects of various co- and tri-culture ratios on the stemness marker expression of the GBM cells, for the first time.

The GBM microenvironment is highly heterogenous and provides biophysical, biochemical as well as cellular cues to tumor cells and is also responsible for its heightened resistance towards the current treatments.[42] Thus, targeting such cues may provide opportunities for therapeutic intervention. GBM cells are in close contact with the perivascular niche consisting of multiple cellular components, including astrocytes and ECs.[46] Here, we have incorporated these cell types in a MCTS model that is known to provide cell–cell and cell–extracellular matrix (ECM) interactions, which, in turn, mediates the cell phenotype.[24]

In this study, we have utilized U87-MG, a well-established GBM cell line that is widely used in glioma research,[53] to assess the changes in their stemness marker expression when cultured in direct contact with astrocytes and ECs in a MCTS model. The GBM cell line was cultured in the presence of serum to represent a more differentiated phenotype of cells, which is typically characterized by their ability to grow as adherent monolayer and lower expression of stemness markers compared to cells grown in serum-free conditions. In addition, cells grown in serum-free conditions typically grow as tumorspheres and exhibit higher expression of stemness markers.[27,35] We successfully constructed coculture MCTS by keeping the number of tumor cells constant and varying the number of astrocytes/ECs to obtain a wide range of ratios while taking into account previously used *in vitro* ratios[4,22,39,50] as well as the *in vivo* scenario wherein, stromal cells are typically in excess compared to tumor cells.[47] In all the coculture conditions, the spontaneous arrangement of cells resulted in loosely aggregated spheroids by day 1 and the compactness of the coculture MCTS increased with time (Fig. S5). The initial decrease in the spheroid sizes for the higher coculture ratios could be attributed to the spheroidization time, wherein the spheroids become compact first and only once the cell–cell adhesions occur, they start to proliferate thereby increasing the spheroid size.[7,52] This observation was specific for coculture spheroids and not GBM-only monoculture spheroids, where there was an increase in the size of the spheroid with time, as previously observed.[19,29,31] In the GBM-only monoculture spheroids, spheroids with lower number of cells exhibited higher growth over time as compared to spheroids with higher number of cells. This has been previously observed in ovarian[16] and pancreatic[25] cancer spheroids. Interestingly, despite the differences in the initial cell seeding density of cells in coculture spheroids, similar sizes of spheroids for almost all conditions (except 1:9) were observed by day 4 itself, and for all the conditions (1:1, 1:2, 1:4 and 1:9; GBM-astrocytes and GBM-EC) at day 7. The loss in the number of stromal cells may be due to the replacement of the astrocytes or ECs by rapidly proliferating tumor cells and has been previously observed in GBM[21] and pancreatic cancer[25] coculture MCTS. This was also indicated by the loss in the green signal due to progressive loss of astrocytes or ECs, which occupied the core of the spheroid over time.

Building on our coculture results, we successfully constructed a triculture MCTS model. To the best of our knowledge, we have utilized GBM cells in combination with astrocytes and ECs in a MCTS model for the first time. This particular combination of GBM cells, astrocytes, and ECs (endothelial umbilical cord blood cells) has been studied just once in a 3D collagen-hyaluronan matrix to study the effects of stromal cells on tumor cell migration, although not in a MCTS model.[18] In our triculture MCTS model, the tumor cells tend to occupy the core with astrocytes and ECs occupying the periphery. This is in contrast to the coculture spheroids where astrocytes or ECs occupy the core. Similar to the coculture MCTS models, spheroidization time was also observed in triculture MCTS. Our results indicate that the structural composition of spheroids in co- and tri-culture MCTS models influence the growth kinetics of the spheroid.

Serum grown U87-MG cells, which typically grow as a monolayer on TCPS represent a more differentiated phenotype.[27] An increased expression of stemness markers such as *SOX2*, *NANOG,* and *OCT4* on culturing U87-MG as 3D spheroids compared to their monolayer counterpart has been observed previously.[51] Also, enhanced expression of stemness markers- *CD133*, *NES*, *SOX2,* and *OCT4* has been previously observed in GBM cells when they were cocultured with astrocytes or HUVECs using 2D

TCPS and 3D scaffolds or hydrogels.[15,22,33,34,43] Herein, we utilized 3D co- and tri-culture MCTS to culture tumor and stromal cells at varying ratios and investigate its impact on the expression of key stemness markers *NES*, *SOX2*, *CD133*, *NANOG*, and *OCT4*. The direct contact between cell types in the co- or tri-culture MCTS altered the stemness expression profile as compared to mixed monoculture MCTS containing each cell type. Ngo et al., used a similar analogy to demonstrate an increase in the malignancy-related genes in GBM cells in triculture with fibroblasts and ECs in 3D gelatin and gelatin-HA hydrogels.[37] More prominent increase in the expression of almost all stemness markers was observed in the higher coculture ratios—1:4 and/or 1:9 in GBM-astrocytes and GBM-EC spheroids. This change was likely mediated by direct cell–cell contact that influences cell–cell signaling and production of growth factors as observed previously,[5,20,33] and persisted even at day 7. For the lower coculture ratios, the stemness marker expression was comparable to the control, indicating that the increased number of astrocytes or ECs enhance the stemness phenotype in a more differentiated population of tumor cells. Our observations are consistent with Kievit et al., who utilized chitosan-alginate scaffolds to coculture U87-MG cells with astrocytes or HUVECs and found increased *CD133* expression in higher stromal cells ratio conditions (i.e., 5:1 compared to 1:1 and 1:5).[22] We also evaluated the percentage of tumor cells positive for the stemness markers through immunofluorescence staining for 1:4 GBM-astrocytes and 1:9 GBM-EC coculture MCTS and these results were largely consistent with qRT-PCR for most of the markers except for NANOG and OCT4 in the case of 1:9 GBM-EC coculture MCTS, and SOX2 and CD133 in the case of 1:4 GBM-astrocytes MCTS. Such discrepancies in the mRNA level and protein expression of stemness markers have been observed previously for glioma cells.[2] Selecting the most influential conditions in the respective coculture models, we constructed a triculture MCTS model with GBM:astrocytes:EC at a ratio of 1:4:9, and observed a prominent increase in the expression of all the stemness markers *via* qRT-PCR. We also performed immunostaining, and our results were largely consistent with qRT-PCR for all the markers except for OCT4. Through immunostaining we observed that although the expression of most of the stemness markers increased, some of them showed no change in expression and this trend has been commonly observed with stemness markers for GBM cells.[2,3,32,44] This might be due to the enrichment of different stemness signatures within the MCTS owing to the culture conditions, in this case—the presence of various stromal cell types.[2] Upregulation of these stemness markers *in vivo* has been correlated with decreased patient survival.[6] Herein, we demonstrated that not only the stromal cell type but also the number of stromal cells in co- or tri-culture with GBM cells influences the stemness marker expression of tumor cells.

Because cancer cell aggregates with diameter between 200 and 500 μm have been known to demonstrate the presence of hypoxic core,[12,45] it is possible that hypoxia could be involved in influencing stemness marker expression. This would be examined in future studies. Overall, such a heterogenous MCTS model can be utilized to investigate the crosstalk between different cell types, however, the following limitations must be taken into account: (a) Based on prior work,[8,26,30,49] murine astrocytes were used in this study; however, future investigations should consider incorporation of human astrocytes. (b) Similarly, based on prior work, HUVECs were used in this study.[4,33,37] However, future studies should consider incorporation of human brain microvascular ECs to enhance the physiological relevance of these models thereby providing a platform for testing therapeutic strategies in the future.

CONCLUSIONS

We successfully constructed 3D co- and tri-culture MCTS models to study the impact of incorporating stromal cells on the growth profile and stemness marker expression of GBM tumor cells. We demonstrated that astrocytes and ECs influenced the stemness marker expression of GBM cells in 3D coculture spheroids, especially in higher coculture conditions with a larger number of astrocytes or ECs compared to tumor cells. Based on these results, we constructed a triculture MCTS model with GBM cells, astrocytes and ECs, and found significant enhancement in the stemness marker expression of tumor cells. Further exploration of the crosstalk between different cell types utilizing such models, would enhance our understanding of the GBM tumor microenvironment, eventually leading to the development of new therapeutic strategies.

SUPPLEMENTARY INFORMATION

The online version contains supplementary material available at https://doi.org/10.1007/s12195-021-00691-y.

ACKNOWLEDGMENTS

This work was supported by the National Science Foundation (CBET 1604677) and the Alabama EPSCoR Graduate Research Fellowship (P.N.). The au-

thors thank Dr. Yuping Bao (University of Alabama) for providing the C8D1A astrocytes and Dr. Matthew Jenny (University of Alabama) for the use of his Nanodrop 2000C spectrophotometer.

CONFLICT OF INTEREST

P. S. Nakod, Y. Kim, and S. S. Rao declare that they have no conflicts of interest.

ETHICAL APPROVAL

No human studies were carried out by the authors for this article. No animal studies were carried out by the authors for this article.

REFERENCES

[1]Akay, M., J. Hite, N. G. Avci, Y. Fan, Y. Akay, G. Lu, and J. J. Zhu. Drug screening of human GBM spheroids in brain cancer chip. *Sci. Rep*. 8:15423, 2018.

[2]Angelucci, C., A. D'Alessio, G. Lama, E. Binda, A. Mangiola, A. L. Vescovi, G. Proietti, L. Masuelli, R. Bei, B. Fazi, S. A. Ciafre, and G. Sica. Cancer stem cells from peritumoral tissue of glioblastoma multiforme: the possible missing link between tumor development and progression. *Oncotarget*. 9:28116–28130, 2018.

[3]Auffinger, B., A. L. Tobias, Y. Han, G. Lee, D. Guo, M. Dey, M. S. Lesniak, and A. U. Ahmed. Conversion of differentiated cancer cells into cancer stem-like cells in a glioblastoma model after primary chemotherapy. *Cell Death Differ*. 21:1119–1131, 2014.

[4]Avci, N. G., Y. Fan, A. Dragomir, Y. M. Akay, and M. Akay. Investigating the influence of HUVECs in the formation of glioblastoma spheroids in high-throughput three-dimensional microwells. *IEEE Trans. Nanobiosci*. 14:790–796, 2015.

[5]Berg, T. J., C. Marques, V. Pantazopoulou, E. Johansson, K. von Stedingk, D. Lindgren, P. Jeannot, E. J. Pietras, T. Bergstrom, F. J. Swartling, V. Governa, J. Bengzon, M. Belting, H. Axelson, M. Squatrito, and A. Pietras. The irradiated brain microenvironment supports glioma stemness and survival via astrocyte-derived transglutaminase 2. *Cancer Res*. 81:2101–2115, 2021.

[6]Bradshaw, A., A. Wickremesekera, H. D. Brasch, A. M. Chibnall, P. F. Davis, S. T. Tan, and T. Itinteang. Cancer stem cells in glioblastoma multiforme. *Front. Surg*. 3:48, 2016.

[7]Cavo, M., D. Delle Cave, E. D'Amone, G. Gigli, E. Lonardo, and L. L. Del Mercato. A synergic approach to enhance long-term culture and manipulation of MiaPaCa-2 pancreatic cancer spheroids. *Sci. Rep*. 10:10192, 2020.

[8]Chen, J. E., J. Lumibao, S. Leary, J. N. Sarkaria, A. J. Steelman, H. R. Gaskins, and B. A. C. Harley. Crosstalk between microglia and patient-derived glioblastoma cells inhibit invasion in a three-dimensional gelatin hydrogel model. *J. Neuroinflammation*. 17:346, 2020.

[9]Chen, W., T. Xia, D. Wang, B. Huang, P. Zhao, J. Wang, X. Qu, and X. Li. Human astrocytes secrete IL-6 to promote glioma migration and invasion through upregulation of cytomembrane MMP14. *Oncotarget*. 7:62425, 2016.

[10]Cheng, V., F. Esteves, A. Chakrabarty, J. Cockle, S. Short, and A. Bruning-Richardson. High-content analysis of tumour cell invasion in three-dimensional spheroid assays. *Oncoscience*. 2:596–606, 2015.

[11]Dahan, P., J. M. Gala, C. Delmas, S. Monferran, L. Malric, D. Zentkowski, V. Lubrano, C. Toulas, E.C.-J. Moyal, and A. Lemarie. Ionizing radiations sustain glioblastoma cell dedifferentiation to a stem-like phenotype through survivin: possible involvement in radioresistance. *Cell Death Dis*. 5:e1543–e1543, 2014.

[12]Daster, S., N. Amatruda, D. Calabrese, R. Ivanek, E. Turrini, R. A. Droeser, P. Zajac, C. Fimognari, G. C. Spagnoli, G. Iezzi, V. Mele, and M. G. Muraro. Induction of hypoxia and necrosis in multicellular tumor spheroids is associated with resistance to chemotherapy treatment. *Oncotarget*. 8:1725–1736, 2017.

[13]Dilnawaz, F., and S. K. Sahoo. Enhanced accumulation of curcumin and temozolomide loaded magnetic nanoparticles executes profound cytotoxic effect in glioblastoma spheroid model. *Eur. J. Pharm. Biopharm*. 85:452–462, 2013.

[14]Dirkse, A., A. Golebiewska, T. Buder, P. V. Nazarov, A. Muller, S. Poovathingal, N. H. C. Brons, S. Leite, N. Sauvageot, D. Sarkisjan, M. Seyfrid, S. Fritah, D. Stieber, A. Michelucci, F. Hertel, C. Herold-Mende, F. Azuaje, A. Skupin, R. Bjerkvig, A. Deutsch, A. Voss-Bohme, and S. P. Niclou. Stem cell-associated heterogeneity in glioblastoma results from intrinsic tumor plasticity shaped by the microenvironment. *Nat. Commun*. 10:1787, 2019.

[15]Fessler, E., T. Borovski, and J. P. Medema. Endothelial cells induce cancer stem cell features in differentiated glioblastoma cells via bFGF. *Mol. Cancer*. 14:157, 2015.

[16]Gunay, G., H. A. Kirit, A. Kamatar, O. Baghdasaryan, S. Hamsici, and H. Acar. The effects of size and shape of the ovarian cancer spheroids on the drug resistance and migration. *Gynecol. Oncol*. 159(2):563–572, 2020.

[17]Hemmati, H. D., I. Nakano, J. A. Lazareff, M. Masterman-Smith, D. H. Geschwind, M. Bronner-Fraser, and H. I. Kornblum. Cancerous stem cells can arise from pediatric brain tumors. *Proc. Natl Acad. Sci. U.S.A*. 100:15178–15183, 2003.

[18]Herrera-Perez, R. M., S. L. Voytik-Harbin, J. N. Sarkaria, K. E. Pollok, M. L. Fishel, and J. L. Rickus. Presence of stromal cells in a bioengineered tumor microenvironment alters glioblastoma migration and response to STAT3 inhibition. *PLoS ONE*. 13:e0194183, 2018.

[19]Hong, X., K. Chedid, and S. N. Kalkanis. Glioblastoma cell line-derived spheres in serumcontaining medium versus serum-free medium: a comparison of cancer stem cell properties. *Int. J. Oncol*. 41:1693–1700, 2012.

[20]Ishiguro, T., H. Ohata, A. Sato, K. Yamawaki, T. Enomoto, and K. Okamoto. Tumor-derived spheroids: relevance to cancer stem cells and clinical applications. *Cancer Sci*. 108:283–289, 2017.

[21]Khosla, K., C. C. Naus, and W. C. Sin. Cx43 in neural progenitors promotes glioma invasion in a 3D culture system. *Int. J. Mol. Sci*. 21(15):5216, 2020.

[22]Kievit, F. M., K. Wang, A. E. Erickson, S. K. Lan Levengood, R. G. Ellenbogen, and M. Zhang. Modeling the tumor microenvironment using chitosan-alginate scaffolds to control the stem-like state of glioblastoma cells. *Biomater. Sci*. 4:610–613, 2016.

[23]Kondapaneni, R. V., and S. S. Rao. Matrix stiffness and cluster size collectively regulate dormancy versus proliferation in brain metastatic breast cancer cell clusters. *Biomater. Sci.* 8:6637–6646, 2020.
[24]Kyffin, J. A., C. R. Cox, J. Leedale, H. E. Colley, C. Murdoch, P. Mistry, S. D. Webb, and P. Sharma. Preparation of primary rat hepatocyte spheroids utilizing the liquid-overlay technique. *Curr. Protoc. Toxicol.* 81:e87, 2019.
[25]Lazzari, G., V. Nicolas, M. Matsusaki, M. Akashi, P. Couvreur, and S. Mura. Multicellular spheroid based on a triple co-culture: a novel 3D model to mimic pancreatic tumor complexity. *Acta Biomater.* 78:296–307, 2018.
[26]Le, D. M., A. Besson, D. K. Fogg, K.-S. Choi, D. M. Waisman, C. G. Goodyer, B. Rewcastle, and V. W. Yong. Exploitation of astrocytes by glioma cells to facilitate invasiveness: a mechanism involving matrix metalloproteinase-2 and the urokinase-type plasminogen activator–plasmin cascade. *J. Neurosci.* 23:4034–4043, 2003.
[27]Lee, J., S. Kotliarova, Y. Kotliarov, A. Li, Q. Su, N. M. Donin, S. Pastorino, B. W. Purow, N. Christopher, W. Zhang, J. K. Park, and H. A. Fine. Tumor stem cells derived from glioblastomas cultured in bFGF and EGF more closely mirror the phenotype and genotype of primary tumors than do serum-cultured cell lines. *Cancer Cell.* 9:391–403, 2006.
[28]Leung, B. M., S. C. Lesher-Perez, T. Matsuoka, C. Moraes, and S. Takayama. Media additives to promote spheroid circularity and compactness in hanging drop platform. *Biomater. Sci.* 3:336–344, 2015.
[29]Lim, W., H. H. Hoang, D. You, J. Han, J. E. Lee, S. Kim, and S. Park. Formation of size-controllable tumour spheroids using a microfluidic pillar array (muFPA) device. *Analyst.* 143:5841–5848, 2018.
[30]Lin, Q., Z. Liu, F. Ling, and G. Xu. Astrocytes protect glioma cells from chemotherapy and upregulate survival genes via gap junctional communication. *Mol. Med. Rep.* 13:1329–1335, 2016.
[31]Liu, Y. J., Y. C. Ma, W. J. Zhang, Z. Z. Yang, D. S. Liang, Z. F. Wu, and X. R. Qi. Combination therapy with micellarized cyclopamine and temozolomide attenuate glioblastoma growth through Gli1 down-regulation. *Oncotarget.* 8:42495–42509, 2017.
[32]Ma, N. K., J. K. Lim, M. F. Leong, E. Sandanaraj, B. T. Ang, C. Tang, and A. C. Wan. Collaboration of 3D context and extracellular matrix in the development of glioma stemness in a 3D model. *Biomaterials.* 78:62–73, 2016.
[33]McCoy, M. G., D. Nyanyo, C. K. Hung, J. P. Goerger, W. R. Zipfel, R. M. Williams, N. Nishimura, and C. Fischbach. Endothelial cells promote 3D invasion of GBM by IL-8-dependent induction of cancer stem cell properties. *Sci. Rep.* 9:9069, 2019.
[34]Nakod, P. S., Y. Kim, and S. S. Rao. Biomimetic models to examine microenvironmental regulation of glioblastoma stem cells. *Cancer Lett.* 429:41–53, 2018.
[35]Nakod, P. S., Y. Kim, and S. S. Rao. Three-dimensional biomimetic hyaluronic acid hydrogels to investigate glioblastoma stem cell behaviors. *Biotechnol. Bioeng.* 117:511–522, 2020.
[36]Narkhede, A. A., J. H. Crenshaw, D. K. Crossman, L. A. Shevde, and S. S. Rao. An in vitro hyaluronic acid hydrogel based platform to model dormancy in brain metastatic breast cancer cells. *Acta Biomater.* 107:65–77, 2020.
[37]Ngo, M. T., and B. A. C. Harley. Perivascular signals alter global gene expression profile of glioblastoma and response to temozolomide in a gelatin hydrogel. *Biomaterials.* 198:122–134, 2019.
[38]Oraiopoulou, M. E., M. Tampakaki, E. Tzamali, T. Tamiolakis, V. Makatounakis, A. F. Vakis, G. Zacharakis, V. Sakkalis, and J. Papamatheakis. A 3D tumor spheroid model for the T98G Glioblastoma cell line phenotypic characterization. *Tissue Cell.* 59:39–43, 2019.
[39]Pustchi, S. E., N. G. Avci, Y. M. Akay and M. Akay. Astrocytes decreased the sensitivity of glioblastoma cells to temozolomide and Bay 11-7082. Int. J. Mol. Sci. 21(19): 7154, 2020.
[40]Raghavan, S., P. Mehta, E. N. Horst, M. R. Ward, K. R. Rowley, and G. Mehta. Comparative analysis of tumor spheroid generation techniques for differential in vitro drug toxicity. *Oncotarget.* 7:16948–16961, 2016.
[41]Rao, S. S., J. J. Lannutti, M. S. Viapiano, A. Sarkar, and J. O. Winter. Toward 3D biomimetic models to understand the behavior of glioblastoma multiforme cells. *Tissue Eng. Part B Rev.* 20:314–327, 2014.
[42]Rape, A., B. Ananthanarayanan, and S. Kumar. Engineering strategies to mimic the glioblastoma microenvironment. *Adv. Drug Deliv. Rev.* 79–80:172–183, 2014.
[43]Rath, B. H., J. M. Fair, M. Jamal, K. Camphausen, and P. J. Tofilon. Astrocytes enhance the invasion potential of glioblastoma stem-like cells. *PLoS ONE.* 8:e54752, 2013.
[44]Raysi Dehcordi, S., A. Ricci, H. Di Vitantonio, D. De Paulis, S. Luzzi, P. Palumbo, B. Cinque, D. Tempesta, G. Coletti, G. Cipolloni, M. G. Cifone, and R. Galzio. Stemness marker detection in the periphery of glioblastoma and ability of glioblastoma to generate glioma stem cells: clinical correlations. *World Neurosurg.* 105:895–905, 2017.
[45]Riffle, S., and R. S. Hegde. Modeling tumor cell adaptations to hypoxia in multicellular tumor spheroids. *J. Exp. Clin. Cancer Res.* 36:102, 2017.
[46]Schiffer, D., L. Annovazzi, C. Casalone, C. Corona, and M. Mellai. Glioblastoma: microenvironment and niche concept. *Cancers (Basel).* 11(1):5, 2018.
[47]Tang, M., Q. Xie, R. C. Gimple, Z. Zhong, T. Tam, J. Tian, R. L. Kidwell, Q. Wu, B. C. Prager, Z. Qiu, A. Yu, Z. Zhu, P. Mesci, H. Jing, J. Schimelman, P. Wang, D. Lee, M. H. Lorenzini, D. Dixit, L. Zhao, S. Bhargava, T. E. Miller, X. Wan, J. Tang, B. Sun, B. F. Cravatt, A. R. Muotri, S. Chen, and J. N. Rich. Three-dimensional bioprinted glioblastoma microenvironments model cellular dependencies and immune interactions. *Cell Res.* 30:833–853, 2020.
[48]Tunici, P., L. Bissola, E. Lualdi, B. Pollo, L. Cajola, G. Broggi, G. Sozzi, and G. Finocchiaro. Genetic alterations and in vivo tumorigenicity of neurospheres derived from an adult glioblastoma. *Mol. Cancer.* 3:25, 2004.
[49]Wei, Z., S. Kale, R. El Fatimy, R. Rabinovsky, and A. M. Krichevsky. Co-cultures of glioma stem cells and primary neurons, astrocytes, microglia, and endothelial cells for investigation of intercellular communication in the brain. *Front. Neurosci.* 13:361, 2019.
[50]Yang, N., T. Yan, H. Zhu, X. Liang, L. Leiss, P. O. Sakariassen, K. O. Skaftnesmo, B. Huang, D. E. Costea, P. O. Enger, X. Li, and J. Wang. A co-culture model with brain tumor-specific bioluminescence demonstrates astrocyte-induced drug resistance in glioblastoma. *J. Transl. Med.* 12:278, 2014.
[51]Yilmazer, A. Evaluation of cancer stemness in breast cancer and glioblastoma spheroids in vitro. *3 Biotech.* 8:390, 2018.

[52]Zanoni, M., F. Piccinini, C. Arienti, A. Zamagni, S. Santi, R. Polico, A. Bevilacqua, and A. Tesei. 3D tumor spheroid models for in vitro therapeutic screening: a systematic approach to enhance the biological relevance of data obtained. *Sci. Rep*. 6:19103, 2016.
[53]Zeng, Y., X. Wang, J. Wang, R. Yi, H. Long, M. Zhou, Q. Luo, Z. Zhai, Y. Song, and S. Qi. The tumorgenicity of glioblastoma cell line U87MG decreased during serial in vitro passage. *Cell Mol. Neurobiol*. 38:1245–1252, 2018.
[54]Zhao, W., Y. Li, and X. Zhang. Stemness-related markers in cancer. *Cancer Transl. Med*. 3:87–95, 2017.